Detecting thermal rectification

Cheng-Li Chiu,[1,2] Chi-Hsun Wu,[1,2] Bor-Woei Huang,[1] Chiao-Ying Chien,[1] and Chih-Wei Chang[1,a]

[1]*Center for Condensed Matter Sciences, National Taiwan University, Taipei 10617, Taiwan*
[2]*Department of Physics, National Taiwan University, Taipei 10617, Taiwan*

Thermal rectification is a special heat transfer phenomenon that thermal conductance of a sample is higher in one direction than that in the reversed direction. Thermal rectifiers have been proposed to be the building blocks of phononic circuits, high performance thermoelectric devices, and energy-saving materials. Theoretically, thermal rectification has been suggested to be ubiquitous, occurring in wherever nonlinear interactions and broken inversion symmetry are present. However, currently available experimental methods have limited sensitivities and are unable to unravel the interesting effect in many systems. Here, by adopting the concept of nonlinear optics, we propose an improved experimental method to detect minuscule thermal rectification from large background thermal conductance. Experimentally, a SiC nanowire, a SiGe nanowire, and a multiwall BN nanotube are investigated and found their thermal rectification is smaller than 0.2% even after asymmetric mass-loading. The method would be very powerful in revealing interesting phonon properties of many materials. *© 2016 Author(s). All article content, except where otherwise noted, is licensed under a Creative Commons Attribution (CC BY) license (http://creativecommons.org/licenses/by/4.0/).* [http://dx.doi.org/10.1063/1.4968613]

In the quest for controlling heat flow in materials has prompted researchers to look for new thermal properties going beyond traditional domains of thermal conduction. Thermal rectification is a special phenomenon that a system displays higher thermal conductance when the temperature gradient is along one particular direction (forward-biased) but lower when it is reverse-biased. The effect of thermal rectification (R) can be quantified as

$$R = \frac{K_{\text{fw}}}{K_{\text{rev}}} \tag{1}$$

where K_{fw} and K_{rev} is the thermal conductance when the sample is forward-biased and reverse-biased, respectively. Similar to the electric diodes in electronics, thermal rectifiers are considered to be one of the building blocks for manipulating heat flow.[1]

While thermal rectification can be anticipated when the heat conduction is dominated by electrons of an electric diode, the realization in a pure phononic system is a hot research topic in recent years.[1] Because the operation of a thermal rectifier would violate reciprocal relation, aside from magnetic systems, it is known that nonlinear interactions and broken inversion symmetries are two necessary conditions for realizing $R>1$.

Historically, thermal rectification as large as $R=2$ was claimed in interfaces of various dissimilar materials and found to be sensitive to external loading, surface roughness, and surface oxidation.[2–6] Apart from the spurious results from experimental artifacts,[7–9] some of the observation were attributed to thermal strain or thermal constriction that led to dissimilar contact areas at forward and reverse biases.[10,11] Later, thermal rectification was claimed to occur in inhomogeneously-doped GaAs though the subtle roles of temperature inhomogeneity or contact thermal resistance were not ruled out in the experiment.[12]

---

[a]Email: cwchang137@ntu.edu.tw

6, 121901-1

In recent years, the interests of thermal rectification based on phononic systems were resurrected by Terrano *et al* using a three-segment nonlinear model.[13] Then there were many theoretical improvements showing that higher R can be obtained in a two-segment configuration or employing different mechanisms.[14–20] Many theoretical works based on engineering real materials have been proposed to reach higher R's.[21–32] Recently, the concept of thermal rectification has been extended to acoustic systems and radiation heat transfer.[33,34]

During the past decade, $R\sim1.07$ in a pure phononic system was observed in BN nanotubes.[35] Later, there were many experiments reporting $R=1.1$ in electronic quantum dots at low temperatures,[36] $R=1.1$ and $R=3$ in nonlinear radiation heat transfer,[37,38] $R=1.21$ in graphene oxides,[39] $R=1.28$ in VO_2 microbeams at phase transition,[40] $R=1.43$ in cobalt oxides of different temperature-dependent thermal conductivities,[41] $R=1.7$ in phonon transmission in patterned Si membrane,[42] and $R=140$ in a metal-superconductor hybrid.[43] It must be emphasized that although proving non-reciprocity is a prerequisite for observing thermal rectification,[44] some experiments may not satisfy the prerequisite due to technical difficulties. Thus, some of the previous experimental findings might not be genuine thermal rectifiers. Furthermore, many theoretical models have suggested that thermal rectification could be omnipresent in nonlinear systems lacking inversion symmetries,[45] but the fundamental question remains to be answered by experiments.

Searching for thermal rectification in many systems thus requires substantial improvements on the measurement sensitivities. In previous experimental works, thermal rectification was obtained via applying a given heat and measuring the thermal conductance at forward and reverse biases, i.e.

$$\begin{cases} P_{fw} = K_{fw}\Delta T_{fw} \\ P_{rev} = K_{rev}\Delta T_{rev} \end{cases} \qquad (2)$$

where P is the applied heat power, ΔT is the temperature difference across the sample, and the subscripts denote forward bias and reverse bias, respectively. In the past, the experimental procedures for switching from forward bias to reverse bias often introduced unwanted perturbations. In addition, the experimental uncertainties of P and ΔT also reduce the sensitivities of $R = K_{fw}/K_{rev} = P_{fw}\Delta T_{rev}/P_{rev}\Delta T_{fw}$. However, there are many challenges in improving the experimental sensitivity. For example, in experiments that P_{fw} and P_{rev} are determined by resistive heating, the non-uniformities of the resistance as well as the unknown temperature profiles of the heater are systematic errors that could significantly affect the sensitivities in measuring R. Even if laser heating is employed in the experiment, the absorption coefficients of the optical transducers are usually poorly measured, and larger uncertainties may result if the three-dimensional temperature distributions are uncertain in the forward and reverse biases. To overcome the issues, controlled experiments on a reference sample assuming $R=1$ are needed. For example, pristine BN nanotubes were assumed to have symmetric results before mass-loading in the previous experiment.[35] Alternatively, background thermal radiation is sometimes used as a reference, assuming to obey symmetric thermal conduction. However, these assumptions are usually not justified. Indeed, while the traditional methods may not have problems in detecting large R's, they become impractical when one is searching for small thermal rectification (i.e. $R-1<0.01$) out of the large background thermal conductances.

Thus a new method must be invented to improve the sensitivity in measuring R. We first note that a system displaying symmetric thermal conduction should display P vs. ΔT relation like Fig. 1(a). If the thermal conductance of the system is temperature dependent (i.e. $K=K_0+aT$), the P vs. ΔT relation would follow Fig. 1(b) and (c) for positive ($a>0$) and negative ($a<0$) temperature coefficients, respectively. On the other hand, for a system exhibiting thermal rectification, the P vs. ΔT relation would display Fig. 1(d–f) for zero, positive, and negative temperature coefficients, respectively. Importantly, the above results show that whenever a system exhibits thermal rectification, P is an asymmetric function of ΔT, whereas the temperature dependent thermal conductance would give P to be an antisymmetric function (i.e. odd function) of ΔT.

The results remind us the fundamental principles of nonlinear optics, in which second harmonic generation is an even function of an applied field and it exclusively occurs in noncentrosymmetric potentials. On the other hand, third harmonic generation is an odd function of an applied field and it only happens in centrosymmetric potentials. Because of the unique sensitivity to systems lacking
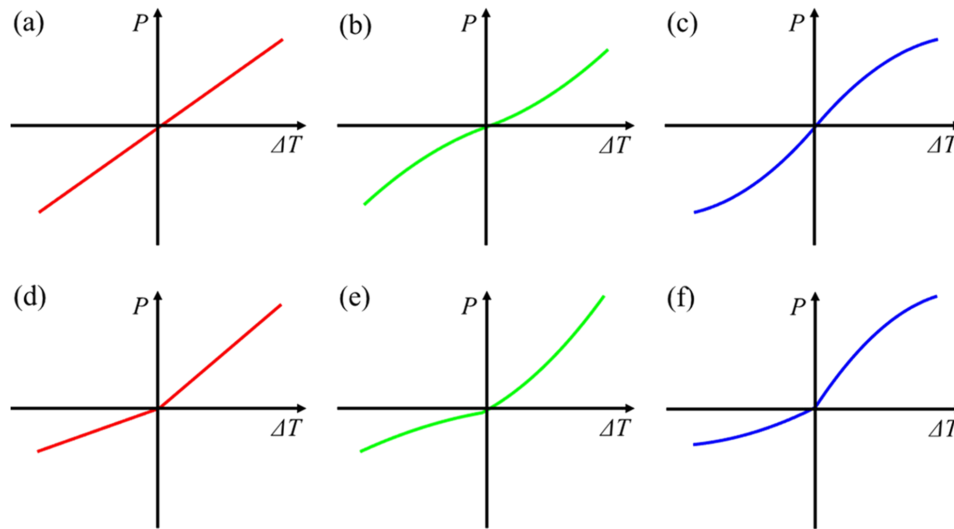
FIG. 1. (a-c) P vs. ΔT relations for symmetric thermal conductors (a) without temperature dependencies, (b) with positive temperature coefficient, and (c) with negative temperature coefficient. Here P is always an antisymmetric function (i.e. odd function) of ΔT. (d-f) P vs. ΔT relations for thermal rectifiers (d) without temperature dependencies, (e) with positive temperature coefficient, and (f) with negative temperature coefficient, showing that P is an asymmetric function (i.e. neither even nor odd function) of ΔT.

inversion symmetries, the second harmonic generation has become a very powerful tool for detecting physical/chemical properties at interfaces regardless of the large optical backgrounds. In analogy to nonlinear optics, we here establish the methods capable of detecting minuscule thermal rectification in thermal systems.

We consider an experimental setup that a sample is sandwiched in between a heater and a sensor. The heater and sensor are respectively connected to a heat bath via a weak thermal link. Without loss of generalities, we consider a resistive heater whose temperature ($T_h(t)$) is controlled by Joule heating of an AC current ($I_0 sin\omega t$) at the heater. On the other hand, the sensor is a resistive sensor whose resistance is a linear function of its temperature. Additionally, the temperature of the sensor ($T_{s,DC}$) is controlled by a DC current ($I_{s,DC}$) at the sensor. The heat generated at the heater will transfer through the sample, resulting in a temperature oscillation at the sensor, following $K_b(T_{s,DC} - T_{bath}) = K_b\delta T_{s,DC} = K(T_h(t) - T_{s,DC}) = K[(I_0 sin\omega t)^2 R_h/K_h - I_{s,DC}^2 R_s/K_s]$ (where T_{bath} is the temperature of the bath, K_b and K are the thermal conductance of the weak link and the sample, R_h and R_s are the resistance of the heater and sensor, K_h and K_s are the resistance of the heater and sensor, respectively).

When $T_h(t) > T_{s,DC}$ (i.e. forward bias) always holds, the temperature oscillations at the sensor will have a component at frequency 2ω, as shown in Fig. 2(a). When the sensor temperature is further raised by increasing $I_{s,DC}$, reverse bias (i.e. $T_h(t) < T_{s,DC}$) may occur at certain time, as shown in Fig. 2(b). If the system exhibits thermal rectification, the 2ω signals at the sensor will be distorted, resulting in a non-zero component at frequency 4ω. In fact, the distortion will be largest when $T_{s,DC}/T_{h,max}=0.5$ ($T_{h,max}$ is the maximum temperature of the heater), as shown in Fig. 2(c). Further increasing $T_{s,DC}$ beyond $T_{h,max}/2$ will again reduce the distortion, as shown in Fig. 2(d). Hence, if the sample exhibits thermal rectification, the 4ω signal will continue to increase with increasing $T_{s,DC}$, peak at $T_{s,DC}/T_{h,max}=0.5$, and vanish at $T_{s,DC}/T_{h,max}=1$, as summarized in Fig. 2(e). In principle, similar to the detection of second harmonic generation in nonlinear optics implies noncentrosymmetric potentials, the detection of a peak in the 4ω signal like Fig. 2(e) will give the evidence of thermal rectification of the investigated system.

The basic idea of P being an asymmetric function of ΔT in thermal rectifiers has also prompted us to look for equivalent methods in detecting thermal rectification. Now we consider applying a DC current and an AC current to the heater, $I_{h,DC} + I_0 sin\omega t$, and a DC current to the sensor, $I_{s,DC}$. The
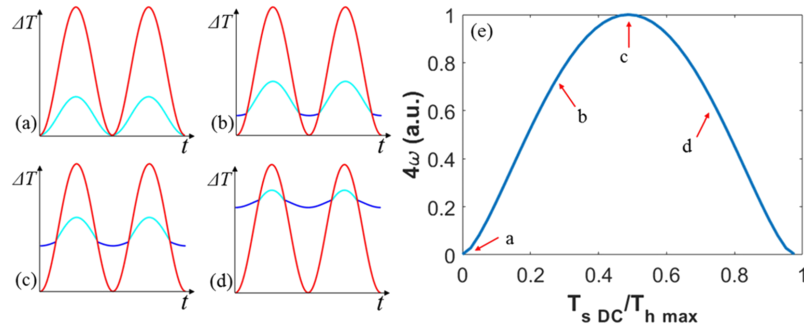
FIG. 2. (a-d) Time dependent temperature variations of the heater (red curves) and the sensor (cyan and blue curves) when gradually raising the temperature of the sensor. The blue curves highlight the distortion when thermal rectification occurs ($R=3$). (e) The distortion will lead to a non-zero signal at frequency 4ω that peaks at $T_{s,DC}/T_{h,max}=0.5$. Here $K=K_{\mathrm{fw}}$ at forward bias and $K=K_{\mathrm{fw}}/3$ at reverse bias.

temperature oscillation at the sensor will follow: $K_b\delta T_{s,DC} = K[(I_{h,DC}+I_0 sin\omega t)^2 R_h/K_h - I_{s,DC}^2 R_s/K_s]$, which has components at 1ω and 2ω frequencies. If the sample is a thermal rectifier, detecting the signals at 1ω and 2ω frequencies at the sensor while scanning $I_{h,DC}$ will give responses shown in Fig. 3(a) and 3(b), respectively. Because the signals at 1ω are proportional to the thermal conductance of the sample, we see that they display a step when changing from forward-bias to reverse-bias, as shown in Fig. 3(a). For the signals at 2ω, they would display a differential of the curve in Fig. 3(a) when $I_0 \ll I_{h,DC}$. As shown in Fig. 3(b), a dip would appear if there is thermal rectification. We also find that the effect of thermal rectification can be easily visualized if plotting $1\omega/2\omega$ signals vs. $I_{h,DC}$, as displayed in Fig. 3(c).

To experimentally test the feasibility of the proposed methods, we employ two Pt film resistors deposited on two suspended SiN_x beams that respectively serve as an independent heater and sensor. Nanotubes or nanowires were picked up by a piezodriven manipulator and anchored to the SiN_x beams by in-situ deposition of Pt/C composites inside an SEM. The thermal conductance (K) of the sample can be obtained by applying Joule heating to the heater and measuring the temperature rises of the heater and sensor. Under steady state, K can be obtained using the relation

$$K = \frac{P}{\Delta T_H - \Delta T_S} \left(\frac{\Delta T_S}{\Delta T_H + \Delta T_S} \right) \tag{3}$$

where P is the Joule heating power, ΔT_H and ΔT_S is the temperature raise on the heater and the sensor, respectively. Due to the linear relation of resistance with respect to temperature of the Pt film resistors, the temperature variations of the heater and the sensor can be directly obtained by measuring their resistance. The temperature calibration was done by measuring their resistance
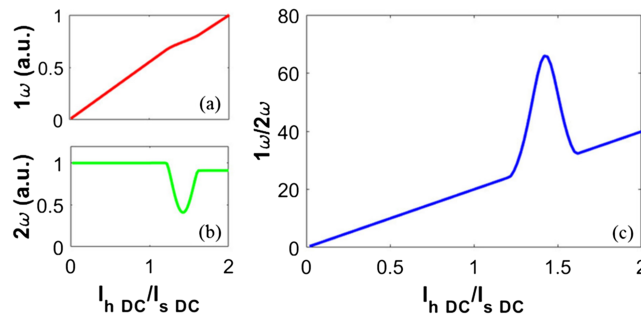

FIG. 3. The signals of a thermal rectifier at (a) 1ω and (b) 2ω frequencies when gradually raising the biased DC current at the heater ($I_{h,DC}$) while the biased current at the sensor ($I_{s,DC}$) is fixed. Distortions of the signal occur when changing from forward-bias to reverse-bias. (c) Normalizing the signals of 1ω to those of 2ω give a linear background with a bump when there is thermal rectification with $R=1.1$.

when uniformly heating the whole device to various known temperatures calibrated by a silicon diode sensor. Experimentally, a Keithley 6221 and a Keithley 224 were respectively employed as AC and DC current sources. A Stanford Research SR830 lock-in amplifier was used for detecting 1ω, 2ω, and 4ω signals. The driving frequencies ($\omega/2\pi$) were generally chosen to be less than 0.8Hz. Similar devices have been employed for measuring thermal conductivities of nanotubes or nanowires in our previous experiments.[35] However, due to the temperature distribution of the heater/sensor beams, the temperature measured here is more like an average temperature rather than the temperature at the ends of the sample. Although numerical corrections can be applied if assuming the quality of the Pt film is uniform along the beam, the assumption is sometimes untenable. Thus the P cannot be accurately determined within 1%. As mentioned earlier, it is a common systematic error which leads to a poorer sensitivity if the traditional method is applied for detecting R.

   Previous discussions on Figs. 1–3 have suggested the 4ω signals to be zero if there is no rectification. In our experiment, we found various effects can contribute a non-zero 4ω signals if an AC heating current ($I_0 sin\omega t$) is applied to the heater. Because the heater power oscillates at 2ω, the following quantities will exhibit temperature oscillations at 2ω as well: (1) temperature dependent of the heater resistance ($R_h(T) = R_{h0} + r sin2\omega t$), (2) temperature dependence of the thermal conductance of the heater ($K_h(T) = K_{h0} + k sin2\omega t$), (3) temperature dependence of the thermal conductance of the sample ($K(T) = a_0 + a sin2\omega t$). Because the sensor temperature is proportional to $K(T)[(I_0 sin\omega t)^2 R_h(T)/K_h(T) - I_{s,DC}^2 R_s/K_s]$, the effects described in (1)-(3) will give non-zero 4ω signals at the sensor temperature. On the other hand, owing to the nonlinear T^4 dependence of radiation heat transfer, effects including (4) radiation heat loss of the heater/sensor to environment, and (5) radiation heat transfer from the heater to the sensor will in general contribute to 4ω signals as well.

   We have incorporated the above effects to simulate our data. It should be emphasized that $R_h(T)$, $K_h(T)$ and $K_{sample}(T)$ are experimentally measured and thermal radiation effects described in (4) and (5) can be determined on a blank device prior to putting a sample. Thus except for the thermal rectification R, no other parameters are used in the analyses. A computer code employing numerical iterations is developed to determine the temperature profile of the heater/sensor beam mentioned above (assuming the quality of the Pt film is uniform along the beam). As shown in Fig. 4(a), we see that when the heater resistance is temperature dependent, the 4ω signals will display a larger background for a good thermal conductor (K=250) than that for a poor thermal conductor (K=1). On the other hand, because the sample's thermal conductance has been normalized in the $1\omega/2\omega$ signals, the backgrounds are insensitive to it, as shown in Fig. 4(b). Importantly, unlike the signature of thermal rectification that always show a peak, we find that if no abrupt changes are present in effects described in (1)-(5), they always display monotonic backgrounds with increasing $T_{s,DC}$. Thus thermal
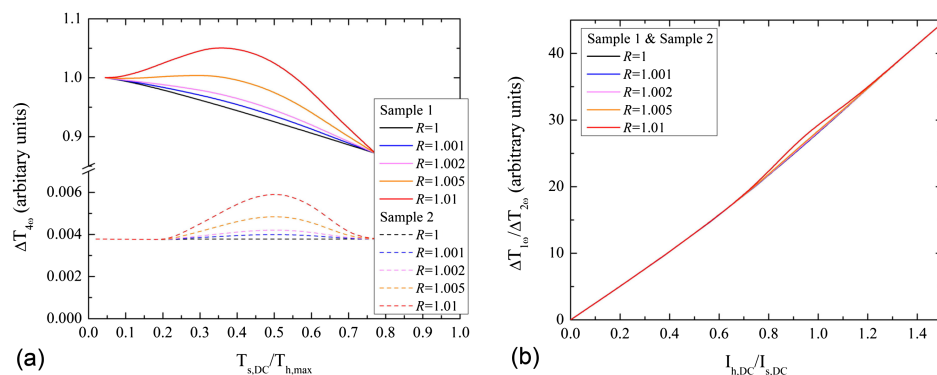

FIG. 4. (a) Simulated 4ω signals for a good thermal conductor (Sample 1, K=250) and a poor thermal conductor (Sample 2, K=1) exhibiting different R's when the heater resistance is temperature dependent. (b) Similar to (a), the corresponding $1\omega/2\omega$ signals for the two samples exhibiting different R's. In the two methods, the backgrounds (R=1) are always found to be monotonic.

rectification, if it exists, would emerge as a peak from the background at around $T_{s,DC}/T_{h,max}$=0.5 and disappear at $T_{s,DC}/T_{h,max}$=1. This feature will allow us to look for the presence of thermal rectification in the following experiments.

We first look for thermal rectification in a pristine SiC nanowire shown in Figs. 5(a). The 4ω signals display a flat line that is independent of the biased $I_{s,dc}$ or $T_{s,DC}$, as shown in Fig. 5(b). From our estimation, we anticipate that a peak would appear at $I_{s,DC} = 15\mu A$ if there is thermal rectification. Following the analyses mentioned above, the absence of a clear peak in Fig. 5(b) indicates R-1<0.5% in the SiC nanowire.

We next look for thermal rectification in a pristine SiGe nanowire shown in the inset of Fig. 6(a). Here the 4ω signals display a non-zero background which decreases with increasing $I_{s,DC}$ (or $T_{s,DC}$), as shown in Fig. 6(a). Regardless of the presence of the background, the absence of a peak at $I_{s,DC} = 16\mu A$ indicates that there is no thermal rectification (R-1<0.2%). The result can be further verified by measuring 1ω and 2ω signals described above. As shown in Fig. 6(b), the $1\omega/2\omega$ signals vs. $I_{h,DC}$ display a linear relation without a bump, which consistently indicate R-1<0.2% in the SiGe nanowire.

Figure 7 shows our measurements on a multiwall BN nanotube before and after mass-loading it by in-situ depositing Pt/C composites at one side of the sample, as shown in Figs. 7(a & b). The 4ω signals display a large background before and after mass-loading but without an appearance of a peak at around $T_{s,DC}/T_{h,max}$=0.5, as shown in Fig. 7(c). The absence of thermal rectification is also confirmed in the $1\omega/2\omega$ signals displayed in Fig. 7(d). Here the $1\omega/2\omega$ signals display a monotonic increasing curve without a bump, indicating R-1<0.2% even with the asymmetric mass-loading. Although the results seem to contradict with the previous experiment on BN nanotubes,[35] it should be noted that the diameter (d=100nm) of the multiwall nanotube investigated here is much larger than previous ones ($d\sim$30nm), which could render the effect of mass-loading to be much less effective.
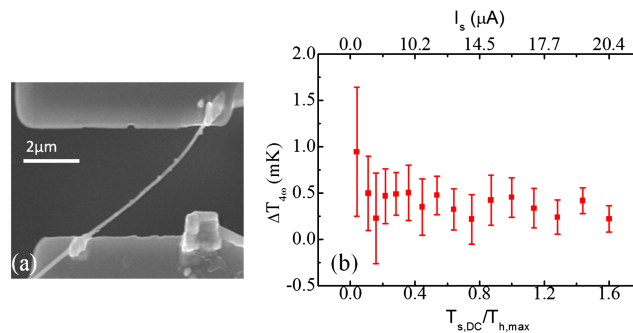

FIG. 5. (a) SEM image of a SiC nanowire anchored between a heater and a sensor. (b) The signals at 4ω when gradually raising the temperature of the sensor. From the data and our analyses, we determine R-1<0.5%.
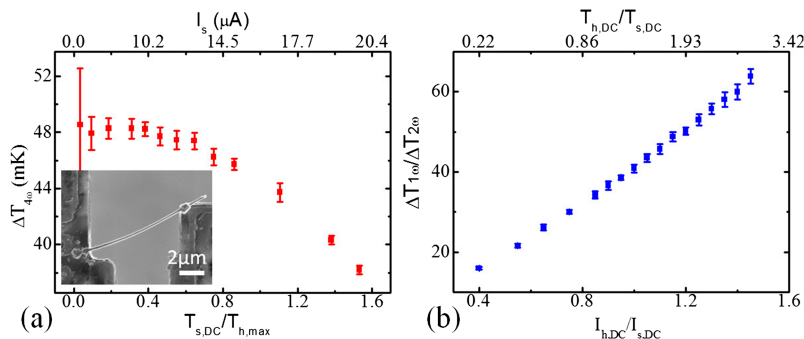

FIG. 6. (a) The signals at 4ω of a SiGe nanowire when gradually raising the $T_{s,DC}$ of the sensor. The inset shows the SEM image of the SiGe nanowire anchored between a heater and a sensor. (b) The $1\omega/2\omega$ signals of the same sample when gradually raising the $T_{h,DC}$ of the heater. From the data and our analyses, we determine R-1<0.2%.
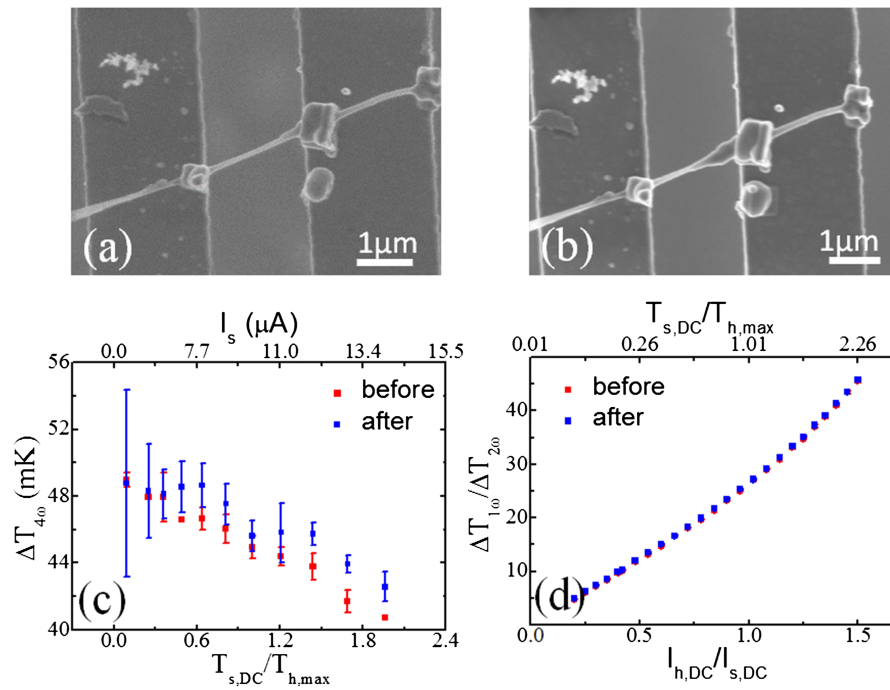
FIG. 7. (a & b) SEM images of a BN nanotube before (a) and after (b) deposition of Pt/C composite on the right side of the nanotube. (c) The signals at 4ω before (red) and after (blue) the deposition. (d) The $1\omega/2\omega$ signals before (red) and after (blue) the deposition. From the data, we determine R-1<0.2%.

Nevertheless, the measurement methods employed here do not rely on any unjustified assumptions; so they are much more rigorous and sensitive than previous methods.

In summary, inspired by the analogy of second harmonic generation in nonlinear optics, we have proposed and demonstrated an improved experimental method for detecting thermal rectification. The method is based on that thermal rectification contributes an asymmetric function to the P vs. ΔT relation and is sensitive to systems exhibiting broken inversion symmetries. Both 4ω and $1\omega/2\omega$ methods are proposed for detecting thermal rectification. Experimentally, we have applied the methods to a pristine SiC nanowire, a pristine SiGe nanowire, and a mass-loaded multiwall BN nanotube. No clear thermal rectification is observed in these samples so far, i.e. R-1<0.2% in the investigated nanowires and the nanotube. The method would be very useful for unraveling interesting phonon properties of nanomaterials, thin films, or bulk crystals.

ACKNOWLEDGMENTS

[1] N. B. Li, J. Ren, L. Wang, G. Zhang, P. Hanggi, and B. W. Li, Rev. Mod. Phys. **84**, 1045 (2012).
[2] C. Starr, Physics **7**, 14 (1936).
[3] M. E. Barzelayk, K. N. Tong, and G. F. Hollowa, NACA TN **3295** (1955).
[4] G. F. C. Rogers, Int. J. Heat Mass Tran. **2**, 150 (1961).
[5] P. W. Ocallaghan, S. D. Probert, and A. Jones, J Phys D Appl Phys **3**, 1352 (1970).
[6] A. Jezowski and J. Rafalowicz, Phys Status Solidi A **47**, 229 (1978).
[7] F. H. Horn. General Electric Rep. No. RL-556 (1951).
[8] A. Williams, Int. J. Heat Mass Tran. **3**, 159 (1961).
[9] R. W. Powell, R. P. Tye, and B. W. Jolliffe, Int. J. Heat Mass Tran. **5**, 897 (1962).
[10] A. M. Clausing, Int. J. Heat Mass Tran. **9**, 791 (1966).
[11] J. R. Barber, Int. J. Heat Mass Tran. **14**, 751 (1971).
[12] C. Marucha, J. Mucha, and J. Rafalowicz, Phys Status Solidi A **31**, 269 (1975).
[13] M. Terraneo, M. Peyrard, and G. Casati, Phys. Rev. Lett. **88**, 094302 (2002).
[14] B. W. Li, L. Wang, and G. Casati, Phys. Rev. Lett. **93**, 184301 (2004).

[15] B. W. Li, J. H. Lan, and L. Wang, Phys. Rev. Lett. **95**, 104302 (2005).

[16] D. Segal and A. Nitzan, Phys. Rev. Lett. **94**, 034301 (2005).

[17] J. H. Lan and B. W. Li, Phys. Rev. B **74**, 214305 (2006).

[18] G. Casati, C. Mejia-Monasterio, and T. Prosen, Phys. Rev. Lett. **98**, 104302 (2007).

[19] E. Pereira, Phys. Rev. E **83**, 031106 (2011).

[20] J. Wang, E. Pereira, and G. Casati, Phys. Rev. E **86**, 010101 (2012).

[21] G. Wu and B. W. Li, Phys. Rev. B **76**, 085424 (2007).

[22] J. N. Hu, X. L. Ruan, and Y. P. Chen, Nano Lett. **9**, 2730 (2009).

[23] M. Alaghemandi, F. Leroy, E. Algaer, M. C. Bohm, and F. Muller-Plathe, Nanotechnology **21**, 075704 (2010).

[24] K. Takahashi, M. Inoue, and Y. Ito, Jpn J Appl Phys **49**, 02bd12 (2010).

[25] D. M. Leitner, Journal of Physical Chemistry B **117**, 12820 (2013).

[26] S. Pal and I. K. Puri, Nanotechnology **25**, 8 (2014).

[27] R. Rurali, X. Cartoixa, and L. Colombo, Phys. Rev. B **90**, 5 (2014).

[28] Y. Wang, A. Vallabhaneni, J. N. Hu, B. Qiu, Y. P. Chen, and X. L. Ruan, Nano Lett. **14**, 592 (2014).

[29] X. Cartoixa, L. Colombo, and R. Rurali, Nano Lett. **15**, 8255 (2015).

[30] Y. Li, X. Y. Shen, Z. H. Wu, J. Y. Huang, Y. X. Chen, Y. S. Ni, and J. P. Huang, Phys. Rev. Lett. **115**, 195503 (2015).

[31] T. Zhang and T. F. Luo, Small **11**, 4657 (2015).

[32] R. Dettori, C. Melis, R. Rurali, and L. Colombo, J. Appl. Phys. **119**, 6 (2016).

[33] B. Liang, B. Yuan, and J. C. Cheng, Phys. Rev. Lett. **103**, 104301 (2009).

[34] C. R. Otey, W. T. Lau, and S. H. Fan, Phys. Rev. Lett. **104**, 154301 (2010).

[35] C. W. Chang, D. Okawa, A. Majumdar, and A. Zettl, Science **314**, 1121 (2006).

[36] R. Scheibner, M. Konig, D. Reuter, A. D. Wieck, C. Gould, H. Buhmann, and L. W. Molenkamp, New J. Phys. **10**, 083016 (2008).

[37] Z. Chen, C. Wong, S. Lubner, S. Yee, J. Miller, W. Jang, C. Hardin, A. Fong, J. E. Garay, and C. Dames, Nat. Commu. **5**, 5 (2014).

[38] K. Ito, K. Nishikawa, H. Iizuka, and H. Toshiyoshi, Appl. Phys. Lett. **105**, 253503 (2014).

[39] H. Tian, D. Xie, Y. Yang, T. L. Ren, G. Zhang, Y. F. Wang, C. J. Zhou, P. G. Peng, L. G. Wang, and L. T. Liu, Sci. Rep. **2**, 523 (2012).

[40] J. Zhu, K. Hippalgaonkar, S. Shen, K. V. Wang, Y. Abate, S. Lee, J. Q. Wu, X. B. Yin, A. Majumdar, and X. Zhang, Nano Lett. **14**, 4867 (2014).

[41] W. Kobayashi, Y. Teraoka, and I. Terasaki, Appl. Phys. Lett. **95**, 171905 (2009).

[42] M. Schmotz, J. Maier, E. Scheer, and P. Leiderer, New J. Phys. **13**, 113027 (2011).

[43] M. J. Martinez-Perez, A. Fornieri, and F. Giazotto, Nature Nanotech. **10**, 303 (2015).

[44] A. A. Maznev, A. G. Every, and O. B. Wright, Wave Motion **50**, 776 (2013).

[45] L. A. Wu, C. X. Yu, and D. Segal, Phys. Rev. E **80**, 041103 (2009).